

uvby – H_β CCD photometry and membership segregation of the open cluster NGC 2548; Gaps in the Main Sequence of open clusters. ^{*}

L. Balaguer-Núñez^{1,2,3}, C. Jordi^{1,4}, D. Galadí-Enríquez⁵

¹ Departament d’Astronomia i Meteorologia, Universitat de Barcelona, Avda. Diagonal 647, E-08028 Barcelona, Spain

² Shanghai Astronomical Observatory, CAS Shanghai 200030, P.R. China

³ Institute of Astronomy, Madingley Road, CB3 0HA Cambridge, UK

⁴ CER for Astrophysics, Particle Physics and Cosmology, associated with Instituto de Ciencias del Espacio-CSIC

⁵ Centro de Astrobiología (CSIC-INTA). Carretera de Ajalvir, km 4, E-28850 Torrejón de Ardoz, Madrid, Spain

Received ; accepted

Abstract. Deep CCD photometry in the *uvby*– H_β intermediate-band system is presented for the cluster NGC 2548 (M 48). A complete membership analysis based on astrometric and photometric criteria is applied. The photometric analysis of a selected sample of stars yields a reddening value of $E(b-y) = 0.06 \pm 0.03$, a distance modulus of $V_0 - M_V = 9.3 \pm 0.5$ (725 pc) and a metallicity of $[\text{Fe}/\text{H}] = -0.24 \pm 0.27$. Through isochrone fitting we find an age of $\log t = 8.6 \pm 0.1$ (400 Myr). Our optical photometry and *JHK* from 2MASS are combined to derive effective temperatures of cluster member stars. The effective temperature distribution along the main sequence of the cluster shows several gaps. A test to study the significance of these gaps in the main sequence of the HR diagram has been applied. The method is also applied to several other open clusters (Pleiades, Hyades, NGC 1817 and M 67) to construct a sequence of metallicities and ages. The comparison of the results of each cluster gives four gaps with high significance (one of them, centred at 4900 K, has not been previously reported).

Key words. Galaxy: open clusters and associations: individual: NGC 2548 – Techniques: photometry – Astrometry – Methods: observational, data analysis, statistical – Stars: Hertzsprung-Russell (HR) and C-M diagrams

1. Introduction

The open cluster NGC 2548 (C0811-056), also known as M 48, in Hydra ($\alpha_{2000} = 8^{\text{h}}13^{\text{m}}48^{\text{s}}$, $\delta_{2000} = -5^\circ 48'$) with an estimated distance of 630 pc (Pesch 1961) or 530 pc (Clariá 1985), is an intermediate-age open cluster, around $\log t = 8.5$ (Lyngå 1987), with a slightly poorer CN abundance than the giants of the Hyades but significantly richer than the K giants of the solar neighborhood (Clariá 1985; Twarog et al. 1997). It has been very poorly studied in spite of being an extended object with an apparent diameter of $30'$ (Trumpler 1930) or even $54'$ (Collinder 1931) and brilliant enough to be in the Messier list (XVIII century) as number 48 (Messier 1850). It was even considered inexistent for several years due to the fact that Messier quoted its coordinates with an error of 5° . Rider et al. (2004) gives

photometry in the Sloan system with a magnitude limit $g' \sim 18$. A recent study by Wu et al. (2005) gives BATC photometry in 13 filters. Radial velocities have been studied by Geyer & Nelles (1985) with a focal reduced spectrograph. They give data for 23 stars but with a very low quality. The only quality measurement is from Wallerstein et al. (1963) of star WEBDA 1560.

This study of NGC 2548 is part of a series of astrometric and photometric analyses of open clusters that follows already published results on NGC 1817 (Balaguer-Núñez et al. 2004a, 2004b) and that will be completed with a study of M 67 (Balaguer-Núñez et al. 2005).

Absolute proper motions of 501 stars within a 1.6×1.6 area in the NGC 2548 region, from automatic MAMA measurements of 10 plates taken with the double astrograph at Zô-Sè station of Shanghai Observatory, were studied by our group (Wu et al. 2002, hereafter Paper I).

In this paper we discuss the results of a deep CCD photometric study of NGC 2548, covering an area of $34' \times 34'$ down to $V \approx 22$. Section 2 contains the details of the CCD observations and their reduction and transforma-

Send offprint requests to: Balaguer-Núñez, L., e-mail: Lola.Balaguer@am.ub.es

^{*} Tables 3, 4 and 5 are only available in electronic form at the CDS via anonymous ftp to cdsarc.u-strasbg.fr (130.79.128.5) or via <http://cdsweb.u-strasbg.fr/cgi-bin/qcat?J/A+A/>

tion to the standard system. In Sect. 3 we discuss a new astrometric membership segregation based on the comparison between parametric and non-parametric approaches applied to the proper motions from Paper I. In Sect. 4 we discuss the colour-magnitude diagram and identify the sample of candidate cluster members using astrometric as well as photometric criteria. Section 5 contains the derivation of the fundamental cluster parameters of reddening, distance, metallicity and age. In Sect. 6 we calculate effective temperatures and study the significance of gaps in the main sequence. The method is also applied to our results on NGC 1817 and NGC 2682 (M 67) and to the well-studied Hyades and Pleiades clusters, allowing us to test the presence of the gaps as a function of age and metallicity. Section 7 summarizes our conclusions.

2. The data

2.1. Observations

Deep Strömgren CCD photometry of the area was performed at the Calar Alto Observatory (Almería, Spain) in January 1999 and January 2000 using the 1.23 m telescope of the Centro Astronómico Hispano-Alemán (CAHA) and in January 1999 and February 2000 using the 1.52 m telescope of the Observatorio Astronómico Nacional (OAN). Further data were obtained at the Observatorio del Roque de los Muchachos (ORM, La Palma, Canary Islands, Spain) in February 2000 using the 2.5 m Isaac Newton Telescope (INT) of ING (equipped with the Wide-Field Camera, WFC), and in December 1998 and February 2000 using the 1 m Jakobus Kapteyn Telescope (JKT) of ING, with the H_β filter. The poor quality of the images obtained in the 1998/99 runs and in the OAN 2000 observations, due to adverse meteorological conditions, prevented us from making use of the data collected during those nights. A log of the observations with the total number of frames, exposure times and seeing conditions is given in Table 1.

We obtained photometry for a total of 4806 stars in an area of $34' \times 34'$ around NGC 2548, down to a limiting magnitude $V \sim 22$. The area covered by the observations is shown in the finding chart of the cluster (Fig. 1). Due to the lack of H_β filter at the WFC-INT, it was only possible to measure it at the JKT and CAHA telescopes, thus limiting the spatial coverage with this filter. Only 283 stars have H_β values. Of those only 253 have values of the rest of the Strömgren filters.

Beside long, deep exposures, additional shorter exposures were obtained in order to avoid saturation of the brightest stars.

2.2. Reduction and transformation to standard system

The reduction of the photometry is explained at length in Balaguer-Núñez et al. (2004b). Our general procedure has been to routinely obtain twilight sky flats for all the filters and a sizeable sample of bias frames (around 10) be-

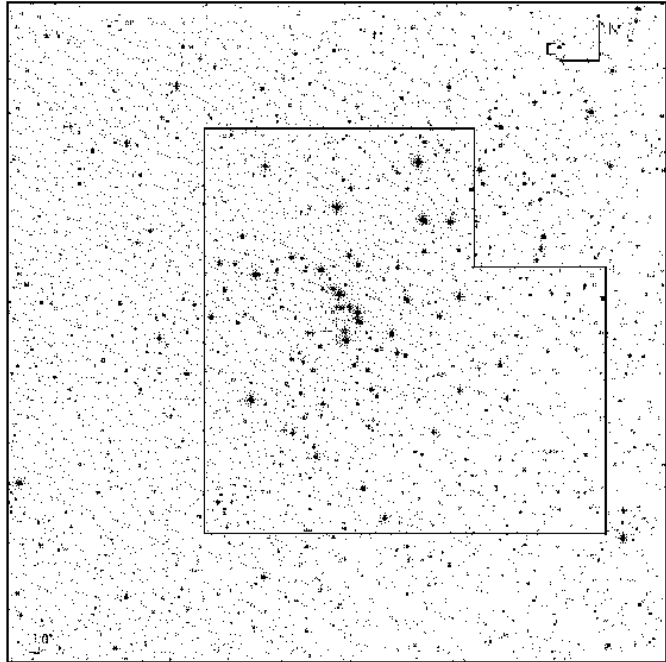


Fig. 1. Finding chart of the area under study. The covered area is marked in black on an image of a plate plotted with Aladin.

fore and/or after every run. Flat fields are typically fewer in number, from five to ten per filter. Two or three dark frames of 2000 s were also taken. IRAF¹ routines were used for the reduction process. The bias level was evaluated individually for each frame by averaging the counts of the most stable pixels in the overscan areas. The 2-D structure of the bias current was evaluated from the average of a number of dark frames with zero exposure time. Dark current was found to be negligible in all the cases. Flatfielding was performed using sigma clipped, median stacked, dithered twilight flats.

Our fields are not crowded. Thus, synthetic aperture techniques provide the most efficient measurements of relative fluxes within the frames and from frame to frame. We used the appropriate IRAF packages, and DAOPHOT and DAOGROW algorithms (Stetson 1987, 1990). We analyzed the magnitude growth curves and determined the aperture correction with the IRAF routine MKAPFILE.

For the WFC images from the INT, we employed the pipeline specifically developed by the Cambridge Astronomical Survey Unit. The process bias subtracts, gain corrects and flatfields the images. Catalogues are generated using algorithms described in Irwin (1985). The pipeline gives accurate positions in right ascension and declination linked to the USNO-2 Catalogue (Monet et al. 1998), and instrumental magnitudes with their corresponding errors. A complete descrip-

¹ IRAF is distributed by the National Optical Astronomy Observatories, which are operated by the Association of Universities for Research in Astronomy, Inc., under cooperative agreement with the National Science Foundation.

Table 1. Log of the observations

Telescope	Date	Seeing(")	n. of frames	Exp.		Times (sec)		H_β
				u	v	b	y	
1.23 m CAHA	1999/01/12-15	(1)	13	1900	800	400	400	2000
1.23 m CAHA	2000/01/05-10	1.1	21	2200	1400	900	800	1400
1.52 m OAN	1999/01/13-16	(1)	15	1900	800	400	400	2000
1.52 m OAN	2000/02/07-14	(1)	5	-	-	-	-	1400
1 m JKT	1998/12/11-14	(1)	26	2000	1200	800	700	1200
1 m JKT	2000/02/02-06	1.1	18	-	-	-	-	2000
2.5 m WFC-INT	2000/02/02-03	1.3	17	2000	2000	1200	500	-

(1) Poor weather conditions. Images not used in the final data.

tion can be found in Irwin & Lewis (2001) and in <http://www.ast.cam.ac.uk/~wfcsur/index.php>.

The coefficients of the instrumental-to standard transformation equations were computed by a least squares method using the instrumental magnitudes of the standard stars and their standard magnitudes and colours in the $uvby - H_\beta$ system. Up to 68 standard stars from the cluster M 67 (Nissen et al. 1987) were observed depending on the size of the field. Four to six short exposures in every filter were taken every night with a magnitude limit of $V=18$. Those standard stars with residuals greater than 2σ were rejected. Typically that involves a 10-15% of the standard stars, mainly variables from the M 67 field. The reduction was performed for each night independently and in two steps. The first step is to determine the extinction coefficients for each passband from the standard stars. With the extinction coefficients fixed, the transformation coefficients to the standard system were fitted.

The mean errors as a function of apparent visual magnitude are given in Table 2 for the NGC 2548 stars.

Table 3 lists the u, v, b, y, H_β data for all 4806 stars in a region of $34' \times 34'$ around the open cluster NGC 2548 (Fig. 1). Star centres are given in the frame (x, y) and equatorial $(\alpha_{J2000}, \delta_{J2000})$ coordinates. An identification number was assigned to each star following the order of increasing right ascension. Column 1 is the ordinal star number; columns 2 and 3 are α_{J2000} and δ_{J2000} ; columns 4 and 5 are the respective x, y coordinates in arcmin; columns 6 and 7 are the $(b - y)$ and its error, 8 and 9 the V magnitude and its error, 10 and 11 the m_1 and its error, 12 and 13 the c_1 and its error, and 14 and 15 the H_β and its error. In column 16, stars considered candidate members (see Sect. 4.1.) are labelled 'M', while those classified as non-members show the label 'NM'.

The cross-identification of stars in common with the astrometry (Paper I), WEBDA (<http://obswww.unige.ch/WEBDA>), Hipparcos (ESA, 1997), Tycho-2 (Høg et al. 2000) and USNO-2 (Monet et al. 1998) catalogues is provided in Table 4.

2.3. Comparison with previous photometry

Only three stars in the NGC 2548 area have been previously studied using Strömgren photometry (WEBDA 0366, 1560, 2156). Unfortunately, none of them is inside the area covered by our photometry. Only one of them (WEBDA 1560) is considered a cluster member from our astrometry and will be studied in Sect. 5.

The V magnitude derived from the y filter can be compared with the published broadband data. There are 30 stars in common with Pesch (1961). The corresponding mean difference in V , in the sense ours minus Pesch's is -0.01 ± 0.03 .

Transformations between $B - V$ and $b - y$ from several authors (see Moro & Munari, 2000) fails to cover the whole range under study. We can find a linear relation between the two indices: $B - V = (1.632 \pm 0.031)(b - y) - (0.038 \pm 0.010)$, $N=30$. The standard deviation of the residuals about the mean relation is 0.048, where the typical uncertainty in $B - V$ is 0.02 and in $b - y$ is 0.016.

3. Astrometric analysis

Paper I gives absolute proper motions of 501 stars within a $1^\circ 6' \times 1^\circ 6'$ area in the NGC 2548 region up to $B_{\text{inst}} \approx 14$, from automatic MAMA measurements of 10 plates and a maximum epoch difference of 82 years. Membership determination is calculated in Paper I with a 9-parametric Gaussian model and a list of stars with a probability higher than 0.7 gives 165 cluster members.

NGC 2548 is a very extended object with a complex structure with a double core, prolate shape and a tidal tail with a clump (Bergond et al. 2001). It has been suggested that this secondary clump is associated with the last strong disk shock that occurred between 20 and 40 Myr ago. Confirmation of members at large radii will trace the distribution of stars that are currently leaving the cluster. This will help to constrain models of the tidal disruption of open clusters.

To complement the cluster/field segregation analysis of the astrometry from Paper I we have applied a non-parametric method to the proper motion data, as explained in Balaguer-Núñez et al. (2004a). In the non-parametric approach we are able to differentiate the clus-

Table 2. Number of stars observed (N) and mean internal errors (σ) as a function of apparent visual magnitude.

V range	V		$(b - y)$		m_1		c_1		H_β	
	N	σ	N	σ	N	σ	N	σ	N	σ
8-9	3	0.019	3	0.028	2	0.016	2	0.002	2	0.017
9-10	19	0.012	19	0.011	19	0.013	16	0.019	5	0.003
10-11	25	0.014	25	0.016	25	0.016	24	0.010	6	0.009
11-12	32	0.012	31	0.013	31	0.018	31	0.016	10	0.030
12-13	45	0.012	43	0.013	43	0.016	43	0.011	12	0.017
13-14	71	0.012	71	0.015	69	0.020	69	0.017	17	0.027
14-15	152	0.012	152	0.023	146	0.029	146	0.030	29	0.016
15-16	260	0.015	260	0.034	259	0.047	251	0.047	42	0.025
16-17	380	0.022	380	0.043	376	0.061	360	0.063	53	0.033
17-18	514	0.030	514	0.035	501	0.043	468	0.043	51	0.036
18-19	639	0.027	639	0.028	592	0.031	477	0.032	8	0.046
19-20	752	0.012	752	0.015	702	0.022	383	0.038		
20-21	859	0.023	859	0.028	662	0.048	160	0.052		
21-22	763	0.049	763	0.063	262	0.089	21	0.082		
22-23	222	0.095	222	0.122	28	0.139				
Total	4736		4733		3717		2451		235	

ter population without the need for any a priori knowledge. Following Galadí-Enríquez et al. (1998), we can perform an empirical determination of the probability density functions (PDFs) evaluating the observed local density in each node of a two-dimensional grid in the vector point diagram (VPD), with a normal circular kernel. The smoothing parameter h (Gaussian dispersion) is chosen using Silverman’s rule (1986). The procedure was tested for several subsamples applying different proper motion cutoffs. Satisfactory results are obtained with a proper motion cutoff of $|\mu| \leq 15 \text{ mas yr}^{-1}$.

The empirical frequency function determined from the VPD corresponding to the area occupied by the cluster is made up of two contributions: cluster and field. To differentiate the two populations we need to estimate the field distribution. For this purpose, we studied the VPD for the plate area outside a circle centered on the cluster. The centre of the cluster was chosen as the point of highest spatial density. We did tests with circles of very different radii, searching a reasonable tradeoff between cleanness (absence of a significant number of cluster members) and signal-to-noise ratio (working area not too small). The kernel density estimator was applied in the VPD to these data, yielding the empirical frequency function, for a grid with cell size of 0.2 mas yr^{-1} , well below the proper motion errors.

We finally found that the area outside a circle with a radius of $35'$ centered on the cluster yields a clean frequency function with low cluster contamination and low noise. The empirical frequency functions can be normalized to yield the empirical PDFs for the mixed population (circle), for the field (outside the circle) and for the cluster (non-field) population. Figure 2 displays these three functions. Of course, the field PDF estimated in the outer area cannot be an absolutely perfect representation of the true field PDF in the whole area. This introduces undesired

noise in the frequency function of the cluster, as shown by the negative density values found in several zones and by some positive fluctuations without physical meaning. These negatives values allow us to estimate the typical noise level, γ , present in the result. To avoid meaningless probabilities in zones of low density, we restricted the probability calculations to the stars with cluster PDF $\geq 3\gamma$. The maximum of the cluster PDF is located at $(\mu_\alpha \cos \delta, \mu_\delta) = (-1.2 \pm 0.2, 2.2 \pm 0.2) \text{ mas yr}^{-1}$.

However, this cluster proper motion is different to the value found in Paper I. As discussed by many authors (Galadí-Enríquez et al. 1998 for example) one of the limitations of the parametric approach is the trend of the circular Gaussian distribution, used to fit the cluster, to assume an excessive width to improve the representation of the field distribution. The cluster mean proper motion will then be thus affected. To measure the influence of this effect, we decided to apply the parametric method but to fix the internal velocity dispersion of the cluster at zero. This way the model will assign to the cluster Gaussian distribution a width related only to measurement errors. We then obtained a mean proper motion of $(\mu_\alpha \cos \delta, \mu_\delta) = (-1.10 \pm 0.08, 2.09 \pm 0.08) \text{ mas yr}^{-1}$, in agreement with the cluster proper motion obtained by the non-parametric approach.

The non-parametric technique does not take into account the errors of the individual proper motions, therefore it does not make any particular distinction between bright or faint stars, different epoch spread and so on. However, the FWHM of the empirical cluster PDF provides an estimation of the errors of the distribution. We obtained a FWHM of $\sim 4.2 \pm 0.2 \text{ mas yr}^{-1}$. If the Gaussian dispersion owing to the smoothing parameter $h = 1.44 \text{ mas yr}^{-1}$ is taken into account, this FWHM corresponds to a value of 1.53 mas yr^{-1} . But from Paper I we know that the mean proper motion precision

is 1.18 mas yr^{-1} which gives us an intrinsic dispersion component of 0.97 mas yr^{-1} , (3 km s^{-1} at the distance of 725 pc from Sect. 5), of the same order but slightly lower than the value obtained by the membership determination in Paper I. This indicates that the intrinsic velocity dispersion of the cluster cannot be neglected. Although fixing it to zero improves the determination of the mean motion of the cluster (position of the centre of the fitted Gaussian), the membership probability results are more meaningful taking into account the intrinsic dispersion. In our analysis, we will use the parametric results from Paper I. However, slight differences in the center of the adopted Gaussian do not affect the segregation, since the stars with highest probability of being members are almost the same in both cases.

The cluster membership probability histogram (Fig. 3) shows a clear separation between cluster members and field stars in both approaches: the solid line is the traditional parametric method (from Paper I) while the dotted line is the non-parametric approach. The non-parametric approach to cluster/field astrometric segregation gives us an expected number of cluster members from the integrated volume of the cluster frequency function in the VPD areas of high cluster density, where $\text{PDF} \geq 3\gamma$. This integration predicts that the sample contains 91 cluster members. Sorting the sample in order of decreasing non-parametric membership probability, P_{NP} , the first 91 stars are the most probable cluster members. The minimum value of the non-parametric probability (for the 91-st star) is $P_{NP} = 82\%$. Table 5 lists the P_{NP} for the 501 stars.

There is not an equivalent rigorous way to decide where to set the limit among members and non-members in the list sorted in order of decreasing parametric membership probability, P_P . But, if we accept the size of the cluster predicted by the non-parametric method, 91 stars, we can consider that the 91 stars of highest P_P are the most probable members, according to the results of the parametric technique. The minimum value of the parametric probability from Paper I (for the 91-st star) is $P_P = 92\%$.

With these limiting probabilities ($P_{NP} \geq 0.82$; $P_P \geq 0.92$), we get a 91% (458 stars) agreement in the segregation yield by the two methods. The 43 remaining stars (9%) with contradicting segregation should be carefully studied. Discrepancies among the two approaches are actually expected due to the statistical nature of the methods themselves.

As in Balaguer-Núñez et al. (2004a), to set up a final and unique list, and trying not to reject true members, we accept as probable members of this cluster those stars classified as members by at least one of the two methods. This is equivalent to merging both lists (each with 91 stars) and eliminating duplicated entries. This way we get a list of 118 probable member stars.

As commented on the Introduction, the available information on radial velocities is not accurate nor complete enough to be useful in improving the membership segregation.

We have studied twenty stars in the area of the secondary clump on the tidal tail proposed by Bergond et al. (2001). Only three of them appear to be cluster members. The rest are randomly distributed in the VPD. Because our limiting magnitude for astrometry $B_{\text{inst}} \approx 14$ is brighter than the $B_{\text{cut}} \approx 14.8$ of Bergond et al. (2001), we cannot discard the reality of this clump. Unfortunately, our photometry does not cover this area. Deeper studies will be necessary.

4. Colour-Magnitude diagrams

We use the $Vvs(v-y)$ colour-magnitude diagram for our study. The colour-magnitude diagram based on this colour index defines the main sequence of a cluster significantly better than the traditional $Vvs(b-y)$ diagram (Fig. 4 left and centre). The colour-magnitude diagram of all the stars in the area displays a fairly well-defined main sequence.

4.1. Selection of candidate member stars

Our photometric measurements help to reduce the possible field contamination in the proper motion membership among bright stars, as well as to enlarge the selection of members towards faint magnitudes. Among those astrometric member stars with photometric measurements, we find one star that is not compatible with the sequence of the cluster outlined in the colour-magnitude diagram. Our astrometric segregation of member stars has a limiting magnitude of $V \approx 13$. From this point down to $V = 18$ we construct a ridge line following a fitting of the observational ZAMS (Crawford 1975, 1978, 1979, Hilditch et al. 1983, Olsen 1984) in the $V - (v-y)$ diagram. A selection of stars based on the distance to this ridge line is then obtained. The chosen margin for candidates includes all the stars between $V + 0.5$ and $V - 1$ from the ridge line, as shown in the right panel of Fig. 4. The margins were chosen to account for observational errors and the presence of multiple stars.

This preliminary photometric selection is refined in the colour-colour diagrams (Fig. 5) with the help of the standard relations from the same authors. A final selection of 331 stars in the area is plotted in Fig. 5 as empty circles in the $[m_1] - [c_1]$, $m_1 - (b-y)$, $c_1 - (b-y)$ and $[c_1] - H_\beta$ diagrams.

5. Physical parameters of the cluster

The stars selected as possible cluster members were classified into photometric regions and their physical parameters were determined as explained in Balaguer-Núñez et al. (2004b). The algorithm, described in Masana et al. (2005a) and Jordi et al. (1997), uses *wby* – H_β photometry and standard relations among colour indices for each of the photometric regions of the HR diagram. Absolute magnitude, effective temperature and gravity as well as the corresponding reddening, distance modulus, metallicity and raw spectral type and luminosity class are calcu-

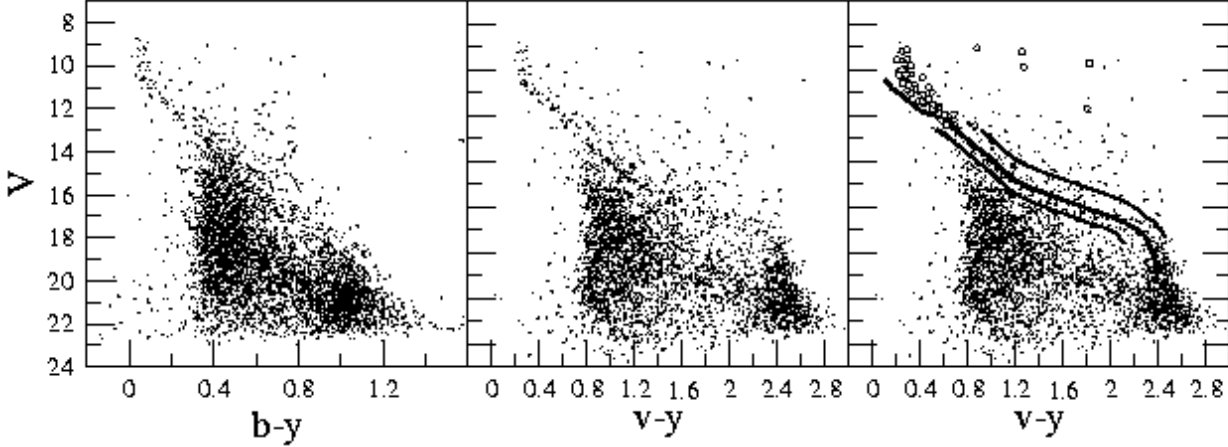


Fig. 4. The colour-magnitude diagram of the NGC 2548 area. Empty circles in the right figure are the astrometric members. Thick line is a shifted ZAMS, with the chosen margin for candidate members ($V + 0.5, V - 1$) in thin lines. See text for details.

lated for each star. Typical errors are 0.25 mag in M_V , 0.15 dex in $[\text{Fe}/\text{H}]$, 270 K in T_{eff} , 0.18 dex in $\log g$ and 0.015 mag in $E(b - y)$.

Only 62 stars among the 331 candidate members have H_β measurements. Thus, the computation of physical parameters is only possible for that subset. The results are shown in Fig. 6. Excluding peculiar stars and those with inconsistencies in their photometric indices and applying an average with a 2σ clipping to that subset, 39 stars remain. We found a reddening value of $E(b - y) = 0.06 \pm 0.03$ (corresponding to $E(B - V) = 0.08$) and a distance modulus of $V_0 - M_V = 9.3 \pm 0.5$ (725 pc, i.e. about 200 pc above the galactic plane). Metallicity is better calculated studying only the 26 F and G stars in our sample following Masana et al. (2005a). We found a value of $[\text{Fe}/\text{H}] = -0.24 \pm 0.27$.

We have examined the bibliography in search of bright stars in the area of NGC 2548 and have found only one compatible with being a member of the cluster: The brightest star (WEBDA 1560), that was saturated in our data. We therefore took its values from Olsen (1993). The stars in the red giant region are detailed in Table 6. Three of them are known spectroscopic binaries. We are cautious about our values of star WEBDA 1218, as the known values of V are 9.64 (Pesch 1961) and 9.63 (Oja 1976), about 0.2 mag brighter. Star WEBDA 0870 was considered to be an astrometric non-member by Ebbinghausen (1939) and in Paper I, while Clariá (1985) studied its weak CN peculiarity and opened the possibility of a cluster member with peculiar composition and proper motion. Star WEBDA 1241 was considered to be a cluster member in Paper I.

The recent publication by Clem et al. (2004) of empirically constrained colour-temperature relations in the Strömgren system enables an isochrone fitting to our results. The best fit is found for the Pietrinferni et al. (2004) tracks. Figure 7 shows isochrones of $[\text{Fe}/\text{H}] = -0.25$

for canonical models (right panel) and for models with overshooting (left panel). Taking into account the number of stars before and after the MS hook, we found a best fit for models with overshooting. The estimated age is of 400 ± 100 Myr ($\log t = 8.6$). Using a different set of tracks by Schaller et al. (1992) we also found agreement with a best estimation of the age of $\log t = 8.6 \pm 0.1$. Neither Pietrinferni et al. (2004) nor Schaller et al. (1992) isochrones provide a perfect fit to the giant members. Similar discrepancies were found by Lapasset et al. (2000) studying the intermediate-age cluster NGC 2539.

Our results are consistent with previous studies. Pesch (1961) gives an $E(B - V) = 0.04 \pm 0.05$ and a distance of 630 pc from UBV photoelectric observations of 30 stars. Clariá (1985) studied DDO photometry of 5 giant stars and gives a value of $E(B - V) = 0.06$ and a distance of 530 pc. Twarog et al. (1997) revised those values and gave an $E(B - V) = 0.05$, a distance of 590 pc and $[\text{Fe}/\text{H}] = 0.08$ from 3 stars. Harris (1976) gives a value of $\log t = 8.28$ from an analysis of nine stars. Høg & Flynn (1998) give $[\text{Fe}/\text{H}] = -0.13$, $E(B - V) = 0.04$ and $\log t = 8.50$ from DDO photometry of three giants. Rider et al. (2004) fix a value $E(B - V) = 0.03$ from bibliography and give values of distance 700 pc, $[Z/Z_\odot] = 0.0$ and an age of 400 Myr by isochrone fitting to $u'g'r'i'z'$ photometry. The recent study by Wu et al. (2005) gives a slightly larger distance (780 pc) and a lower age (0.32 Gyr) also fitting isochrones with $E(B - V) = 0.04$ and solar metallicity. A summary of this information is given in Table 7 for clarity.

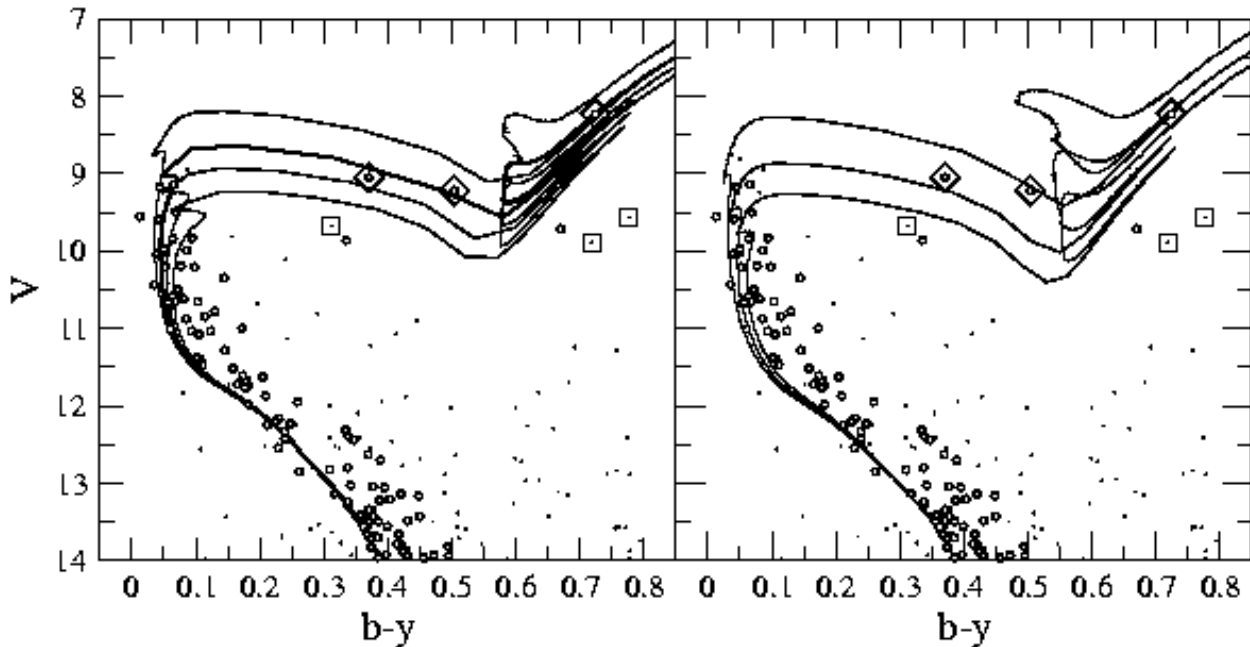
6. Gaps in the Main Sequence

Gaps in the main sequence have been observed and debated for a long time. In the Hyades, de Bruijne et al. (2000) confirmed the reality of two gaps near $B - V \sim 0.38$ and $B - V \sim 0.48$ ($T_{\text{eff}} \sim 6400$ K). Evidence for the existence of gaps among field stars has also been debated

Table 6. Red giants in NGC 2548, with their membership. The first five are from the WEBDA list of Red Giants. Three of them are known spectroscopic binaries.

Phot. Id.	WEBDA	$(b - y)$	V	P_P	P_{NP}	M/NM
1006	0870	0.670 ± 0.0185	9.712 ± 0.0185	0.07	0.84	M?
2556	1218	0.335 ± 0.0370	9.862 ± 0.0305	0.83	0.85	M
2732	1260	0.370 ± 0.0002	9.050 ± 0.0047	0.97	0.84	M SB
2894	1296	0.504 ± 0.0004	9.215 ± 0.0023	0.94	0.86	M SB
(1)	1560	0.724 ± 0.0020	8.199 ± 0.0060	0.88	0.84	M SB
3971	1521	0.312 ± 0.0079	9.671 ± 0.0081	0.00	0.00	NM
4557	1616	0.719 ± 0.0045	9.890 ± 0.0045	0.00	0.00	NM
2645	1241	0.777 ± 0.0072	9.565 ± 0.0072	0.81	0.66	NM?

(1) Photometry taken from Olsen (1993)

**Fig. 7.** Isochrones from Pietrinferni et al. (2004) for scaled solar models of $[\text{Fe}/\text{H}] = -0.25$ and ages of 300, 400, 500, 600 Myr for models with overshooting (left panel) and 200, 300, 400 Myr for canonical models (right panel). Empty circles are candidate members. Red giants are analyzed in detail (see text): diamonds are spectroscopic binaries, squares are astrometric non-members. The adopted reddening and distance modulus are $E(b - y) = 0.06$ and $V_0 - M_V = 9.3$.

(Newberg & Yanny 1998), and recently Kovtyukh et al. (2004) showed a new gap among field stars in the effective temperature range 5560 to 5610 K.

6.1. Method

The characteristics of our photometry and member selection procedure allow us to pursue the search for gaps in the main sequence not only for the previously discussed cluster, NGC 2548 (M 48), but also in the other clusters included in our project: NGC 1817 (Balaguer-Núñez et al. 2004a, 2004b) and NGC 2682 (M 67, Balaguer-Núñez et al. 2005). To check the reliability of the results, we apply the same gap search to the Pleiades (M 45) and the Hyades, two well-known clusters in which gaps have been

previously reported (de Bruijne et al. 2000, Belikov et al. 1998, and specially their Figs. 1 and 3, respectively.)

We estimate effective temperatures for our selection of candidate members following a new approach (Ribas et al. 2003, Masana et al. 2005b) based on fitting observed IR photometry with accurately calibrated synthetic photometry. We use our values of V magnitude and the 2MASS values for J , H , and K magnitudes. The process requires metallicity and surface gravity data that we compute from our Strömgren photometry as explained in previous sections. The method is restricted to the temperature interval from 4000 K to 8000 K, with quoted uncertainties of 0.5-1.3%. The upper temperature limit is due to the increased dependence of the results on the accuracy of $\log g$, while the lower limit is related to the decreasing performance of

Table 7. Comparison of the physical parameters of the cluster with results from other authors. See the text for detailed information of the assumptions made in each case.

Reference	$E(B - V)$ mag	[Fe/H] dex	$\log t$	Distance pc	Comments
This work	0.08	-0.24 ± 0.27	8.6 ± 0.1	725	
Wu et al. (2005)	0.04	0.0	8.51	780	Isochrone fit
Rider et al. (2004)		0.0	8.60	700	Isochrone fit
Høg & Flynn (1998)	0.04	-0.13	8.50		<i>DDO</i> Phot. 3 stars
Harris (1976)			8.28		Phot. 9 stars
Twarog et al. (1997)	0.05	0.08		590	<i>DDO</i> Phot. 3 stars
Clariá (1985)	0.06	0.1		530	<i>DDO</i> Phot. 5 stars
Pesch (1961)	0.04			630	<i>UBV</i> Photoelectric 30 stars

the models because of molecular bands. Ribas et al. (2003) show that, in this range, the procedure is essentially insensitive to the adopted value of [Fe/H] and $\log g$: uncertainties of 0.3 dex in metallicity and 0.5 dex in gravity induce T_{eff} deviations inferior to 0.5%. The number of member stars from our selection of clusters that also have 2MASS photometry in the range of temperatures under study is of 269 stars for NGC 2548, 307 stars for NGC 1817 and 588 stars for NGC 2682. For Pleiades we obtain 225 member stars and for Hyades 76.

After getting the T_{eff} values, we proceeded to the gap search following a method analogous to that proposed by Rachford & Canterna (2000). A simple χ^2 test with one degree of freedom is used to evaluate the significance of any candidate gap. To do this, we take a candidate gap of width W_{in} and we compute the number of stars within it, N_{in} . This number is compared with the stars located on both sides of the gap. We take two bins of equal width, W_{out} , at the sides of the candidate gap, and we count the stars inside them, n_{out} . Then, n_{out} is scaled to the size of the gap to give $N_{\text{out}} = W_{\text{in}} n_{\text{out}} / (2W_{\text{out}})$ and this quantity is compared to N_{in} to get the χ^2 value. To limit the effect of small number statistics, and again following Rachford & Canterna (2000), the computation is done only when at least five stars are present on each side of the gap, which guarantees that $n_{\text{out}} \geq 10$.

We performed this calculation for a grid of gap widths $75 \text{ K} < W_{\text{in}} < 500 \text{ K}$, at intervals of 25 K, and placing the gap centres every 1 K over the intersection of the temperature range covered by the method with the range covered by the photometry. To prevent edge effects, intervals of 300 K were avoided at the extremes of the intersection.

After several trials, we chose $W_{\text{out}} = 100 \text{ K}$ for our photometry, but the Pleiades and Hyades required $W_{\text{out}} = 200 \text{ K}$, due to the smaller size of the photometric sample. It is important to note that widening W_{out} can alter the relative value of χ^2 and its associated probability, but with little effect on the significance of the gap centre position or width.

Having computed χ^2 for the whole range of gap centres and sizes, we selected the local maxima of the resulting table. We observed that changes in W_{in} do not make gaps

appear or disappear, but only affect their significance. All significant gaps have probability values higher than 0.99.

6.2. Results

Table 8 gives the centres and widths (W_{in}) for the significant gaps in the temperature range studied. The two well-known Böhm-Vitense gaps are clearly detected in Hyades and also Pleiades, which serves as a check of the reliability of the method. Both gaps are significant in the whole sample of clusters analysed, with the exception of M 67, due to the much higher age of this stellar system (the main sequence is so evolved that the corresponding effective temperature range is no longer populated).

The gap recently reported by Kovtyukh et al. (2004) in field stars at 5560-5610 K, and already suspected in the Hyades (de Bruijne et al. 2000), stands out not only in the Hyades, but also in the other clusters surveyed. In the case of M 67, Fan et al. (1996) also raised the possible existence of this gap placed around $1 M_{\odot}$.

The reliability of the new gap detected around $T_{\text{eff}} \sim 4900 \text{ K}$ is stressed by its appearance in all the clusters under study with the only exception of NGC 1817. The reason is that, in this case, our photometry does not reach stars colder than 5000 K.

Even though we know that some amount of field contamination is present in our candidate member selection, it is worth noting that the significance of the four gaps in our photometric data is outstanding. If an even more reliable member selection would be possible, this could make the gaps even more evident in our data.

The position and width of the gaps are compared with the age and metallicity of the clusters in Fig. 8. No clear trend can be drawn from this comparison. However, metallicity effects could be masked due to the uncertainties in the metallicity determinations used for NGC 2548, NGC 1817 and NGC 2682 (M 67) that are of the order of 0.2 dex.

Independently of the physical explanation for the existence of these gaps, there is no reason, in principle, to expect them to appear at the same positions and with similar sizes in all the clusters. There can be a com-

Table 8. Gaps in temperature empirically detected in the main sequence of open clusters.

Cluster	Age Gyr	[Fe/H] dex	Centre K	Width K	Centre K	Width K	Centre K	Width K	Centre K	Width K
Pleiades (M 45)	0.1	-0.03	7377	300	6821	325	5577	275	4845	275
NGC 2548 (M 48)	0.4	-0.24	7099	475	6305	425	5465	350	4785	350
Hyades	0.7	0.15	7006	475	6427	250	5452	225	4972	275
NGC 1817	1.1	-0.34	7323	175	6674	350	5701	300	-	-
NGC 2682 (M 67)	4.2	0.01	-	-	-	-	5593	125	5017	200

Table 9. Orientative and approximate characterization of the mean loci of the gaps detected.

$\langle T_{\text{eff}} \rangle$ (K)	$\sigma_{\langle T_{\text{eff}} \rangle}$ (K)	$B-V$	Spec.	Mass (M_\odot)
7200	180	~ 0.30	F0	~ 1.6
6600	230	~ 0.40	F2-F5	~ 1.3
5600	100	~ 0.70	G5-G8	~ 0.80
4900	110	~ 0.90	K2	~ 0.75

plex dependency on metallicity, age and other parameters. However, the clusters studied show some regularity that allows to distinguish, as mentioned, four independent gaps. Even though we know that this kind of average may lack physical meaning, we give a table with mean, approximate parameters that characterize the loci of the four gaps (Table 9). The colour indexes and masses are taken from standard relations (Schmidt-Kaler 1982) and assume solar metallicity.

Several theoretical explanations have been proposed for the three hotter gaps (see the references already given). Most but not all, point to the need to improve the treatment of rotation and convection in stellar models. However, theoretical and/or empirical references to the fourth, colder gap are lacking. Spectroscopy could confirm or reject the reality of this gap whose significance is similar to that of the others, on the basis of our photometric data.

7. Conclusions

In this paper we give a catalogue of accurate Strömgren *uvby* – H_β and J2000 coordinates for 4806 stars in an area of $34' \times 34'$ around NGC 2548.

We give a selection of probable members of NGC 2548, combining the photometric study with an astrometric analysis using parametric as well as non-parametric approaches. An improved determination of the physical parameters of this cluster based on our photometry gives: $E(b - y) = 0.06 \pm 0.03$, $[\text{Fe}/\text{H}] = -0.24 \pm 0.27$, a distance modulus of $V_0 - M_V = 9.3 \pm 0.5$ and an age of $\log t = 8.6 \pm 0.1$. The values are consistent with previous studies (see Chen et al. 2003 and references therein).

We perform a search for possible gaps in the main sequence of this cluster and, also, of the other clusters analysed in our project (NGC 1817, M 67). The Pleiades and Hyades are added as a check and to construct a sequence

of ages and metallicities. We find four gaps in the effective temperature interval 4000–8000 K. The coldest gap, around 4900 K, had not been previously reported.

Acknowledgements. We are grateful to Eduard Masana for very useful discussions and for providing the code for calculating effective temperatures. We would like to thank Simon Hodgkin and Mike Irwin for their inestimable help in the reduction of the images taken at the WFC-INT. L.B.-N. also wants to thank Gerry Gilmore and Floor van Leeuwen for their continuous help and valuable comments, as well as all the people at the IoA (Cambridge) for a very pleasant stay. L.B.-N. gratefully acknowledges financial support from EARA Marie Curie Training Site (EASTARGAL) during her stay at IoA. Based on observations made with the INT and JKT telescopes operated on the island of La Palma by the RGO in the Spanish Observatorio del Roque de Los Muchachos of the Instituto de Astrofísica de Canarias, and with the 1.52 m telescope of the Observatorio Astronómico Nacional (OAN) and the 1.23 m telescope at the German-Spanish Astronomical Center, Calar Alto, operated jointly by Max-Planck Institut für Astronomie and Instituto de Astrofísica de Andalucía (CSIC). This study was also partially supported by the contract No. AYA2003-07736 with MCYT. This research has made use of Aladin, developed by CDS, Strasbourg, France. This publication makes use of data products from the Two Micron All Sky Survey, which is a joint project of the University of Massachusetts and the Infrared Processing and Analysis Center/California Institute of Technology, funded by the National Aeronautics and Space Administration and the National Science Foundation.

References

- Balaguer-Núñez L., Jordi C., & Galadí-Enríquez D., 2005, (in preparation)
- Balaguer-Núñez L., Jordi C., Galadí-Enríquez D., & Zhao J.L., 2004a, *A&A* 426, 819
- Balaguer-Núñez L., Jordi C., Galadí-Enríquez D., & Masana E., 2004b, *A&A* 426, 827
- Belikov A.N., Hirte S., Meusinger H., Piskunov A.E., & Schilbach E., 1998, *A&A* 332, 575
- Bergond G., Leon S., & Guibert J., 2001, *A&A* 377, 462
- Clariá J.J., 1985, *A&AS* 59, 195
- Chen L., Hou J.L., & Wang J.J., 2003, *AJ* 125, 1397
- Clem J.L., VandenBerg D.A., Grundahl F., & Bell R.A., 2004, *AJ* 127, 1227
- Collinder P., 1931, *Lund Observatory Annals* n. 2.
- Crawford D.L., 1975, *AJ* 80, 955

- Crawford D.L., 1978, AJ 83, 48
 Crawford D.L., 1979, AJ 84, 1858
 de Bruijne J.H.J., Hoogerwerf R., & de Zeeuw P.T., 2000, AJ 544, L65
 Ebbighausen E.G., 1939, ApJ 90, 689
 ESA, 1997, The Hipparcos and Tycho Catalogues, SP-1200
 Fan X., Burstein D., Chen J.-S., et al., 1996, AJ 112, 628
 Galadí-Enríquez D., Jordi C., & Trullols E., 1998, A&A 337, 125
 Geyer E.H., & Nelles B., 1985, A&AS 52, 301
 Harris G.L.H., 1976, ApJS 30, 451
 Hilditch R.W., Hill G., & Barnes J.V., 1983, MNRAS 204, 241
 Høg E., Fabricius C., Makarov V.V., et al. 2000, A&A 357, 367
 Høg E., & Flynn C., 1998, MNRAS 294, 28
 Irwin M., & Lewis J., 2001, New Astron. Rev 45, 105
 Irwin M.J., 1985, MNRAS 214, 575
 Jordi C., Masana E., Figueras F., & Torra J., 1997, A&AS 123, 83
 Kovtyukh V.V., Soubiran C., & Belik S.I., 2004, A&A 427, 933
 Lapasset E., Clariá J.J., & Mermilliod J.-C., 2000, A&AS 361, 945
 Lyngå G., 1987, Catalogue of Open Clusters, Centre de Données Stellaires, Strasbourg.
 Masana E., et al. , 2005a, (in preparation)
 Masana E., et al. , 2005b, (in preparation)
 Messier C., 1850, CDT 1784, 227
 Monet, D., Bird A., Canzian, B., et al. 1998, The USNO-A2.0 Catalogue, (U.S. Naval Observatory, Washington DC).
 Moro D., & Munari U., 2000, A&AS 147, 361
 Newberg H.J., & Yanny B., 1998, ApJ 499, L57
 Nissen P.E., Twarog B.A., & Crawford D.L., 1987, AJ 93, 634
 Oja T., 1976, private communication (as quoted in WEBDA)
 Olsen E.H., 1993, A&AS 102, 890
 Olsen E.H., 1984, A&AS 57, 443
 Pesch P., 1961, ApJ 134, 602
 Pietrinferni A., Cassisi S., Salaris M., & Castelli F., 2004, ApJ 612, 168
 Rachford B.L., & Canterna R., 2000, AJ 119, 1296
 Ribas I., Solano E., Masana E., & Giménez A., 2003, A&A 411, 501
 Rider C.J., Tucker D.L., Smith J.A., et al. 2004, AJ 127, 2210
 Schaller G., Schaerer D., Meynet G. & Maeder A., 1992, A&A 96, 269
 Schmidt-Kaler Th., 1982, Landolt-Börstein: Numerical Data and Functional Relationships in Science and Technology, edited by K. Schaifers and H.H. Voigt (Springer-Verlag, Berlin), volume VI, subvolume 2b.
 Silverman B.W., 1986, Density Estimation for Statistics and Data Analysis, J.W. Arrowsmith Ltd.
 Stetson P.B., 1987, PASP 99, 191
 Stetson P.B., 1990, PASP 102, 932
 Trumpler R.J., 1930, Lick Obs. Bull., 14, 154
 Twarog B.A., Ashman K.M., & Anthony-Twarog B.J., 1997, AJ 114, 2556
 Wallerstein G., Westbrooke W., & Hannibal D., 1963, PASP 75, 522
 Wu Z.Y., Zhou X., Ma J., & Chen J.S., 2005, PASP 117, 32
 Wu Z.Y., Tian K.P., Balaguer-Núñez L., et al. 2002, A&A 381, 464 (Paper I)

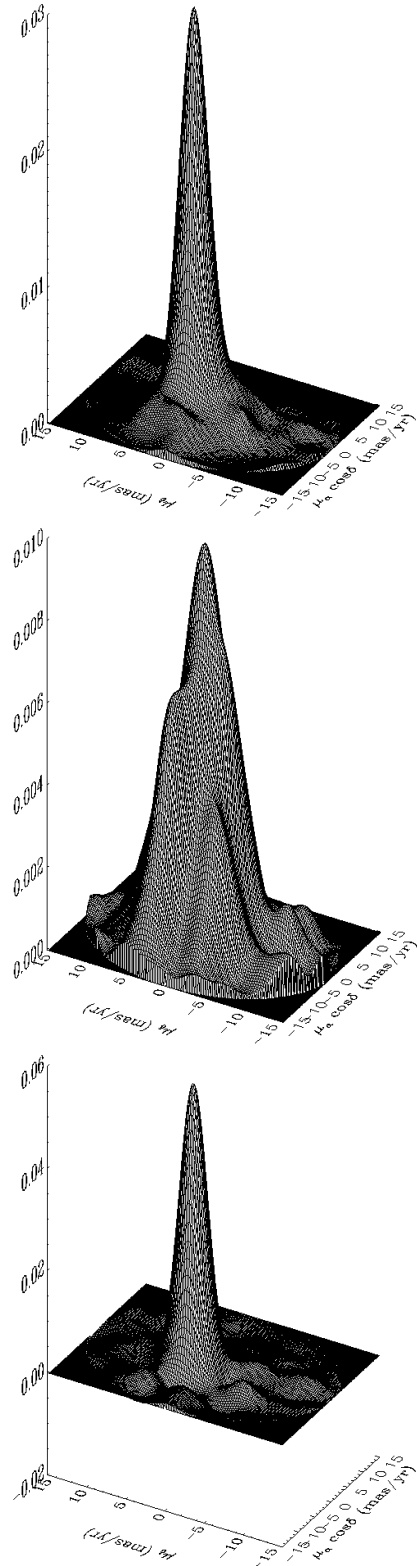


Fig. 2. Empirical probability density functions in the kinematic plane. Top: mixed sample from the inner circle of 35'. Center: field population from outside this circle. Bottom: cluster population of NGC 2548

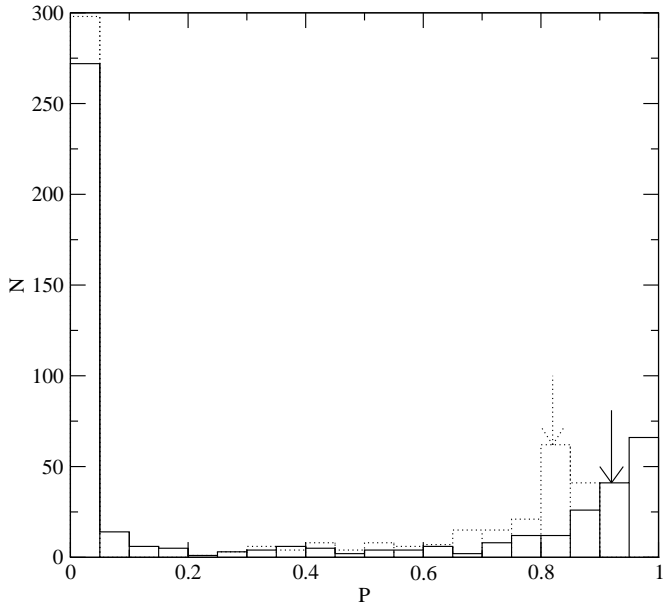


Fig. 3. The histogram of cluster membership probability of NGC 2548. The solid line gives the results for traditional parametric method (Paper I), while the dotted line corresponds to the non-parametric approach. The arrows mark the limiting probabilities for member selection for each method.

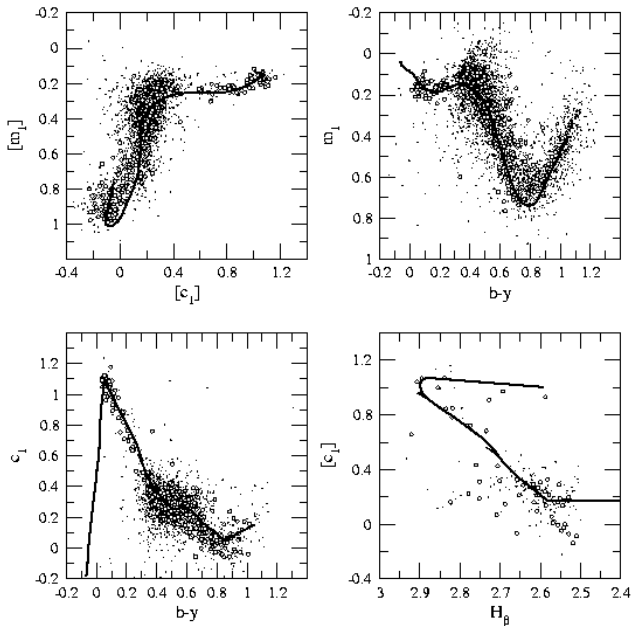


Fig. 5. The colour-colour diagrams of NGC 2548. Empty circles denote candidate members of NGC 2548, chosen with astrometric and non-astrometric criteria as explained in Sect. 4.1. The thick line is the standard relation shifted by $E(b - y) = 0.06$ when necessary.

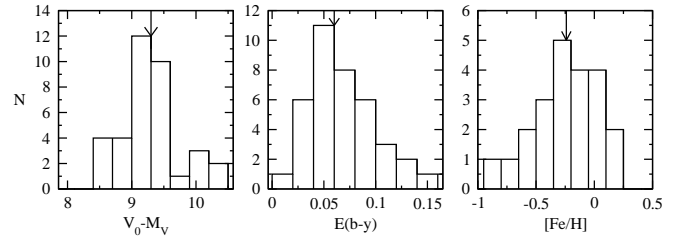


Fig. 6. The histograms of the distance modulus, reddening and metallicity of the selected member stars of NGC 2548 with H_β measurements. The arrows indicate the mean values adopted for the cluster.

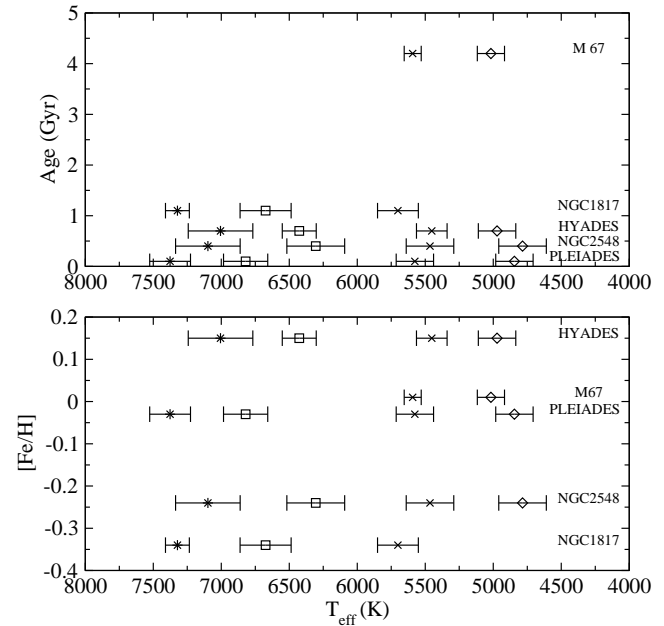


Fig. 8. Gaps in temperature vs. age (upper panel) and metallicity (lower panel). See text for the metallicity uncertainties.